Supplement of Atmos. Chem. Phys., 24, 3729–3742, 2024
https://doi.org/10.5194/acp-24-3729-2024-supplement

Atmospheric Chemistry and Physics
Open Access

Supplement of

Production of oxygenated volatile organic compounds from the ozonolysis of coastal seawater

Delaney B. Kilgour et al.

Correspondence to: Timothy H. Bertram (timothy.bertram@wisc.edu)

S1 Calibrations for Scripps Pier field analysis and associated uncertainties

Calibration factors used for Scripps Pier analysis are in Table S2. All calibration factors except for "Aldehyde" were calibrated in-field or immediately after the field project. All other ions with a positive emission flux were calibrated by scaling the generic aldehyde calibration factor determined during lab ozonolysis experiments to field sensitivities using DMS as a transfer standard. This was done due to the majority of the emission flux ions without a measured molecule-specific calibration factor having the formula $C_xH_y^+$ or $C_xH_yO_z^+$. We acknowledge that the lack of molecule-specific calibration factors and the PTR-ToF-MS not being coupled to a GC for the field experiment introduce uncertainties to the flux quantifications.

The first major source of uncertainty in this analysis is the decision to quantify $C_5H_9^+$ as isoprene. This was done because without a coupled GC for the field experiment, we do not have evidence that isoprene did not contribute to this ion at Scripps Pier. Because it is likely that isoprene along with other molecules contributed to the measurement of this ion in the field and we did not have in-field calibration factors for the other molecules that could contribute to this ion, we chose to use the isoprene calibration factor. This supports that if the emission flux of $C_5H_9^+$ was solely due to isoprene, the implied dissolved isoprene concentrations would be too high, relative to what exists in the literature currently, for this to be plausible. If we instead used the aldehyde calibration factor to quantify $C_5H_9^+$, the measured $C_5H_9^+$ flux would be roughly a factor of 4 lower. As such, we interpret the calibration of $C_5H_9^+$ flux as an aldehyde to represent a lower limit and calibration of $C_5H_9^+$ flux as isoprene to represent an upper limit. In Table S3, we report $\varphi_{VOC,field}$ and the mean emission flux of $C_5H_9^+$ calibrated as isoprene and aldehyde to provide a range.

The second source of uncertainty is the decision to calibrate the non-$C_5H_9^+$ ions measured at Scripps Pier in Table S3 with the aldehyde sensitivity, without having GC measurements to support this molecular identification. This was chosen due to not having other in-field calibration factors to use and them having the same ion formula as the lab experiments where a GC was present. If we instead used the average sensitivity to all 14 molecules calibrated to in-field, we would get a calibration factor of 3.4 cps ppt^{-1}, indicating that the quantification of these ions is a minor source of uncertainty, relative to the existing flux uncertainty.

S2 Calculations for implied waterside dissolved isoprene concentration

Implied waterside dissolved isoprene concentrations were calculated according to the procedure outlined in Kim et al. (2017). A brief summary is provided as follows:

The flux (F) of a molecule across the air-sea interface can be calculated from its concentration in the seawater (C_w), concentration in the gas-phase (C_a), total transfer velocity (K_t), and dimensionless liquid over gas solubility (α) according to Eq. (S1):

$$F = K_t(C_w - \frac{C_a}{\alpha}) \quad \text{(S1)}$$

Based on typical C_a and C_w for isoprene of <300 ppt and 0.1-100 pM (Shaw et al., 2010), respectively, and a Henry's law constant of 0.013 M atm^{-1} (Sander, 2015), isoprene is supersaturated in the waterside, resulting in Eq. (S2):

$$C_w = \frac{F}{K_H K_t} \quad \text{(S2)}$$

K_t was calculated as a function of wind speed using the waterside transfer parameterization of Nightingale et al. (2000) and the airside transfer parameterization of Johnson (2010). Henry's law constants were scaled for a temperature of 20° C and a salinity of 35 PSU.

Step	Duration (min)	V1	V2	N_2 Flow (slpm)	O_2 Flow (slpm)	CO_2 Flow (slpm)	Description
1	60	Off	Off	3.90	0.100	0.0014	N_2/O_2 mixture passed through O_3 generator. O_3 flow is through empty flow tube.
2	2	Off	On	3.90	0.100	0.0014	N_2/O_2 mixture passed through O_3 generator. O_3 flow bypasses empty flow tube. Water is filled in flow tube during this time.
3	45	On	Off	3.20	0.800	0.0014	Zero air flow is through water-filled flow tube.
4	60	Off	Off	3.90	0.100	0.0014	N_2/O_2 mixture passed through O_3 generator. O_3 flow is through water-filled flow tube.

Table S1: Sequence used for flow tube experiments. Durations are approximate.

Ion	Calibrated Molecule	Calibration Factor (cps ppt^{-1})
$C_2H_7S^+$	Dimethyl sulfide	3.9 (Novak et al., 2022)
CH_5S^+	Methanethiol	1.3 (Novak et al., 2022)
$C_5H_9^+$	Isoprene	1.1
$C_4H_9O^+$	Methyl ethyl ketone	5.1
$C_3H_4N^+$	Acrylonitrile	6.2
$C_{10}H_{17}^+$	α-pinene	1.7
$C_8H_{11}^+$	o-xylene	5.0
$C_9H_{13}^+$	1,2,4-trimethylbenzene	4.2
$C_{10}H_{31}O_5Si_5^+$	D5 Siloxane	2.3
$C_7H_9^+$	Toluene	2.5
$C_{10}H_{17}O^+$	β-cyclocitral	4.4
All Other Ions	Aldehyde	4.1

Table S2: Calibration factors used for Scripps Pier analysis.

Ion	Mass	$\varphi_{VOC,lab}$ (%)	$\varphi_{VOC,field}$ (%)	Mean Emission Flux at Scripps Pier (ppt m s^{-1})
$C_5H_9^+$	69.06988	14.1 (11.8-17.3)	2.62 (2.22-3.20)[a] 0.70 (0.60-0.86)[b]	0.12[a] 0.032[b]
$C_5H_{10}^+$	70.0777	0.721 (0.608-0.889)	0.032 (0.027-0.039)	0.0016
$C_6H_9^+$	81.06988	9.19 (7.73-11.3)	0.88 (0.75-1.07)	0.042
$C_6H_{10}^+$	82.0777	0.722 (0.608-0.889)	No flux above flux LOD	No flux above flux LOD
$C_6H_{11}^+$	83.08553	8.66 (7.29-10.7)	0.37 (0.32-0.46)	0.018
$C_6H_{12}^+$	84.09335	0.627 (0.527-0.771)	0.029 (0.024-0.035)	0.0015
$C_7H_{13}^+$	97.10118	8.66 (7.29-10.7)	0.26 (0.22-0.32)	0.013
$C_9H_{13}^+$	121.1012	1.42 (1.19-1.74)	0.29 (0.25-0.35)	0.014
$C_9H_{15}^+$	123.1168	1.58 (1.33-1.95)	0.10 (0.089-0.13)	0.0049
$C_9H_{17}^+$	125.1325	1.10 (0.922-1.35)	0.029 (0.025-0.036)	0.0014
$C_9H_{17}O^+$	141.1274	0.568 (0.478-0.699)	No flux above flux LOD	No flux above flux LOD
$C_9H_{19}O^+$	143.143	2.19 (1.84-2.70)	0.037 (0.031-0.045)	0.0018
$C_9H_{21}O_2^+$	161.1536	1.03 (0.871-1.27)	0.023 (0.019-0.028)	0.0010

Table S3: Ions showing an ozonolysis response in laboratory experiments are listed below. For an ion to qualify, it had to meet the following criteria:

1. **Ozonolysis response measured by the RT-Vocus must be prompt. Maximum value must be reached within 4 and 35 minutes after adding O_3, where 4.3 minutes is the residence time of the flow tube.**
2. **The ion must show this ozonolysis response in >75% of completed experiments.**
3. **The ion signal intensity on the RT-Vocus at the peak must meet the threshold of being >50 cps, at least twice that of the initial signal at t = 0 minutes and at least 1.5 times that of the final signal at t = 60 minutes. This signal threshold was chosen to ensure that data analysis over the entire experiment was above a conservative instrument detection limit.**

Superscripts a and b represent $C_5H_9^+$ calibrated as isoprene and as an aldehyde, respectively.

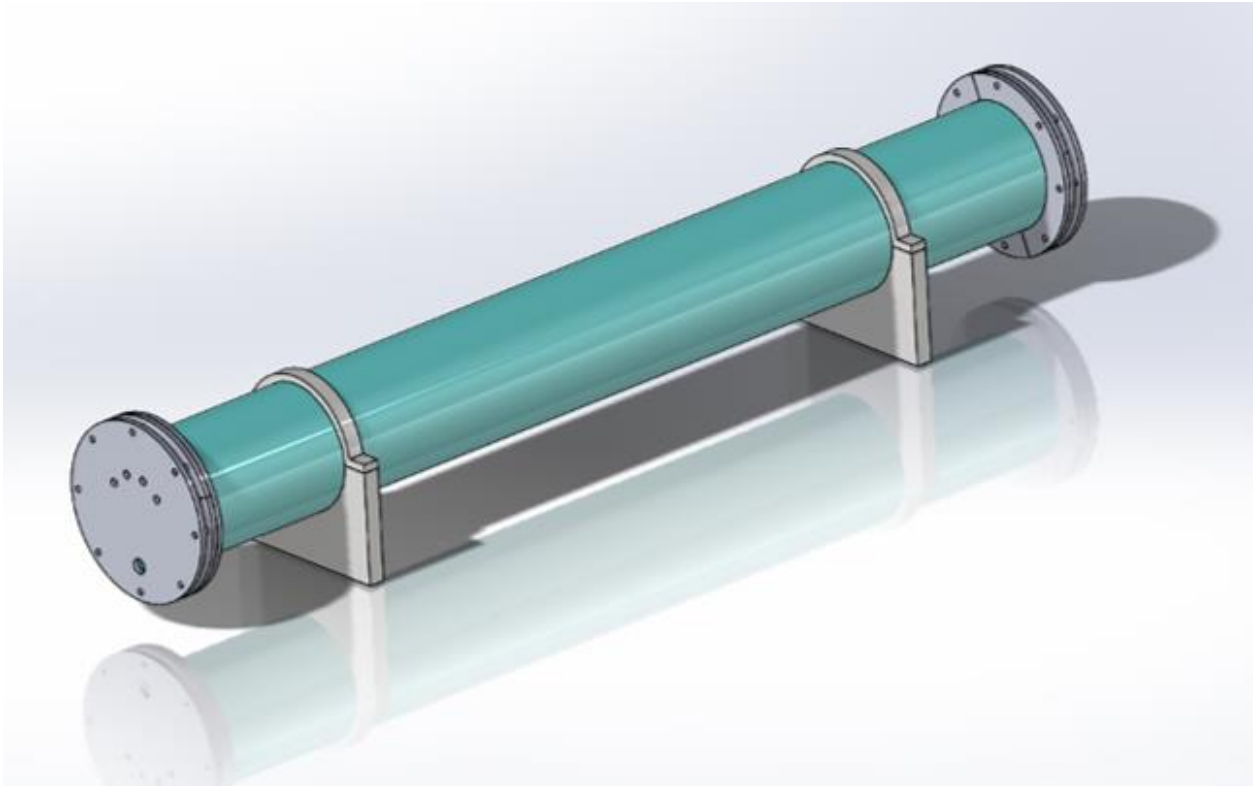

Figure S1: Schematic of the flow tube used for ozonolysis experiments. Water was contained in a quartz glass tube (Technical Glass Products) measuring 122 cm in length and 135 mm in inner diameter. Flanges made of 316 stainless steel were secured to the ends of the tube to provide a gas- and water-tight enclosure. Each flange was fitted with a single ½″ or ¾″ Swagelok fitting used for water and drainage delivery (located at the bottom of the flange pictured) and four ¼″ Swagelok fittings used for headspace gas flow (located at the top of the flange pictured). All but one ¼″ Swagelok fitting on each flange were capped for these experiments.

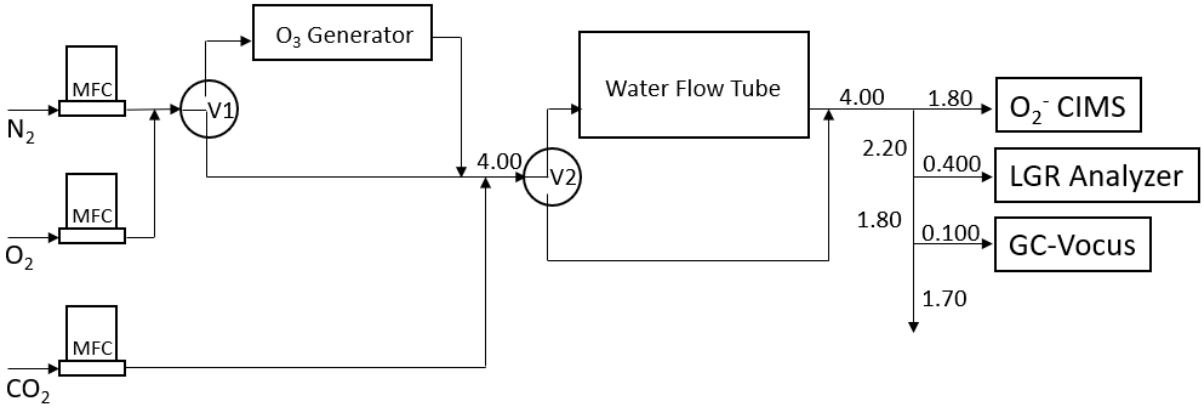

Figure S2: Schematic of the flow tube experimental method described in Table S1. Numeric values represent flow rates in Liters per minute at different points in the flow path. The upward pointing arrows and downward pointing arrows from valves V1 and V2 represent the "off" and "on" positions, respectively, as described in Table S1.

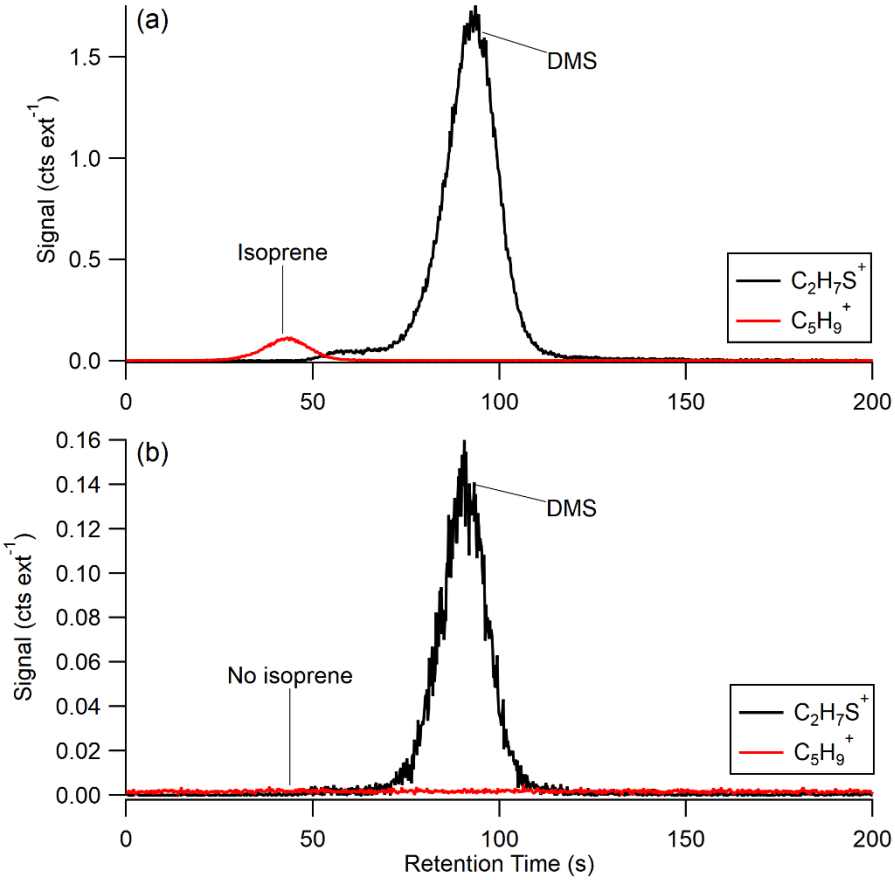

Figure S3: (a) GC-Vocus chromatogram corresponding to DMS and isoprene standards. Isoprene was detected at $C_5H_9^+$ and eluted at 45 seconds and DMS was detected at $C_2H_7S^+$ and eluted at 90 seconds. (b) GC-Vocus chromatogram corresponding to Table S1 Step 3 for seawater showing ions where DMS and isoprene are detected. No biogenic degassing isoprene was observed in these experiments despite the presence of other BVOC, like DMS.

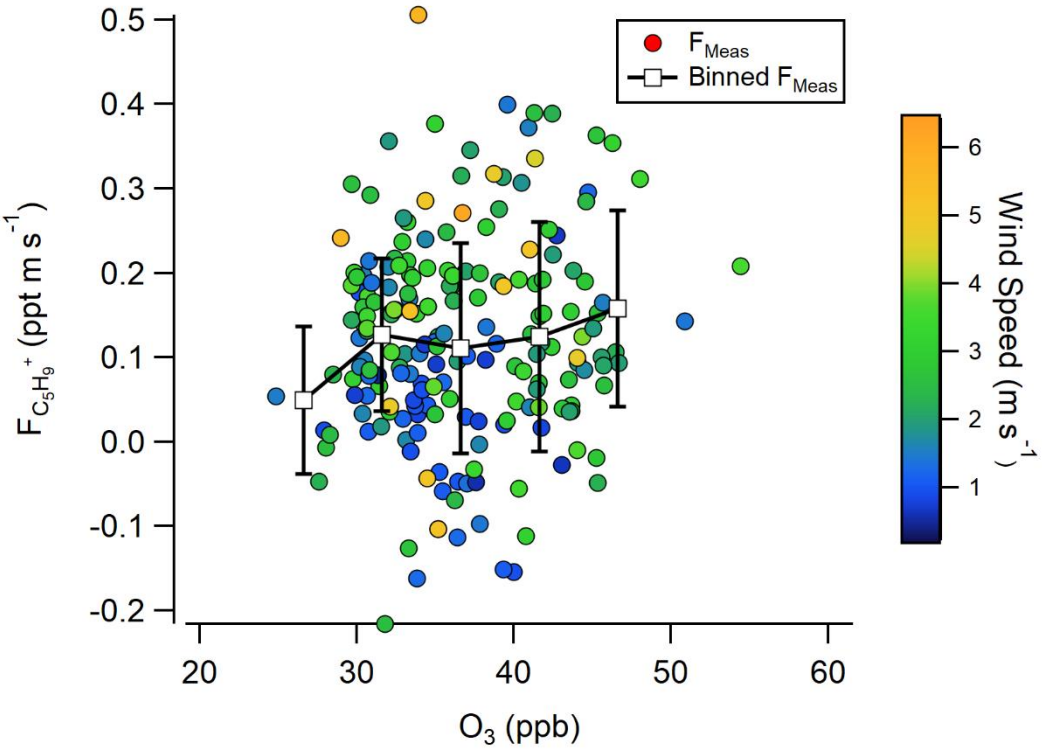

Figure S4: Flux of $C_5H_9^+$ calibrated as isoprene as a function of O_3 mixing ratios measured at Scripps Pier in 2019.

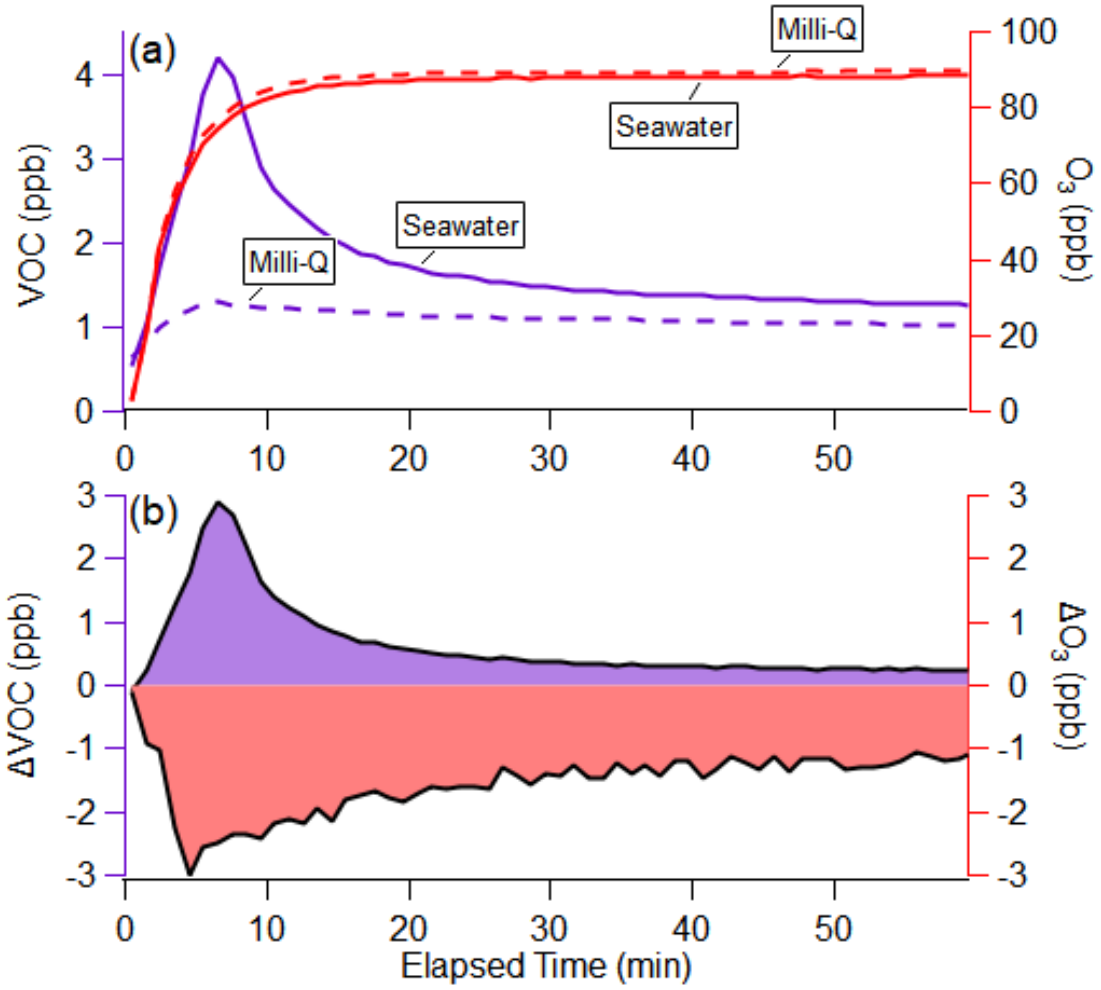

Figure S5: One representative laboratory experiment corresponding to O_3 addition to the flow tube containing water (step 4 of sequence in Table S1). (a) VOC is the sum of signal for all ions in Table S3, calibrated with the average sensitivity of 1.29 cps ppt^{-1}. Total VOC from ozonolysis peaks at 4.2 ppb for the seawater case versus 1.3 ppb for the Milli-Q case. The small rise in VOC in the Milli-Q case from 0-6 minutes is likely a result of small impurities in the water. O_3 is the measured signal by the Ox-CIMS calibrated with the Model 49i Ozone Analyzer. O_3 measured in the seawater case is slightly lower than O_3 measured in the Milli-Q case due to O_3 deposition to salts and DOC in the seawater that are not present in Milli-Q. (b) ΔVOC and ΔO_3 are calculated according to Eq. (1) and Eq. (2), respectively.

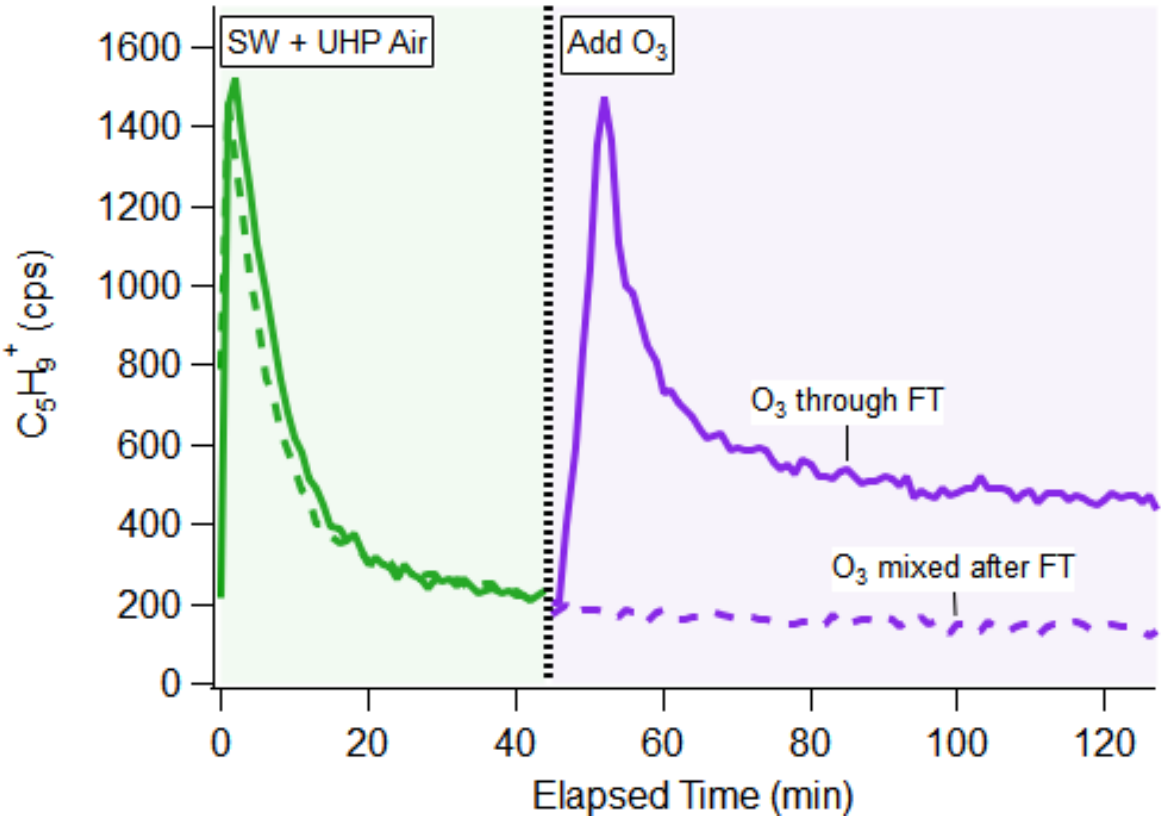

Figure S6: RT-Vocus measurement of $C_5H_9^+$ when ultrapure air is added to a flow tube containing seawater and then O_3 is added to the flow tube containing seawater (solid lines), following steps 3 and 4 of the sequence detailed in Table S1. Dashed lines correspond to RT-Vocus measurement of $C_5H_9^+$ when ultrapure air is added to a flow tube containing seawater (step 3 in Table S1) and then O_3 is added downstream of the flow tube, so O_3 bypasses the flow tube and is only flowing through the tubing after it toward the instrumentation. The lack of prompt ozonolysis response in $C_5H_9^+$ in the dashed line case suggests that the prompt ozonolysis observed in the experiments (as in the solid line case) is not a result of reactions of BVOC in the tubing or Vocus region reacting with O_3 and instead is indicative of ozonolysis of the seawater surface.

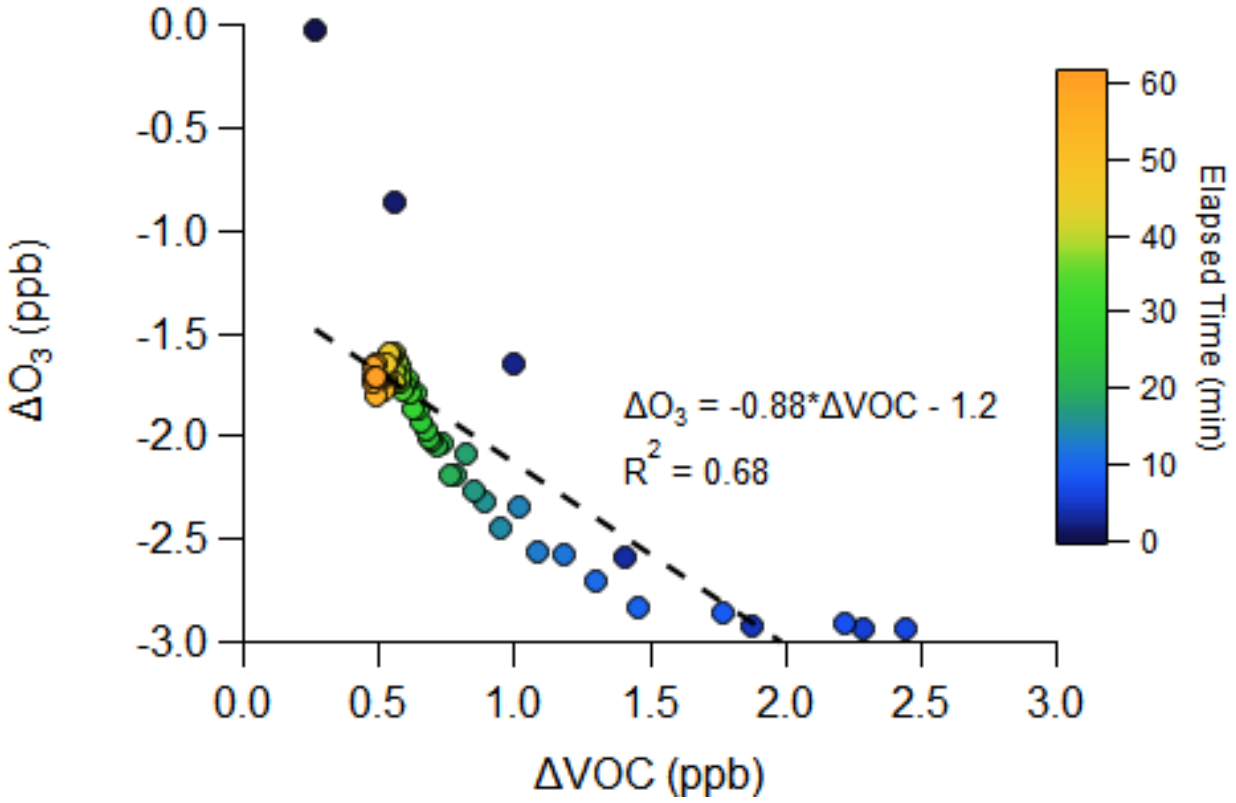

Figure S7: Regression of ΔVOC vs. ΔO_3 for seawater ozonolysis corresponding to step 4 of the sequence in Table S1.

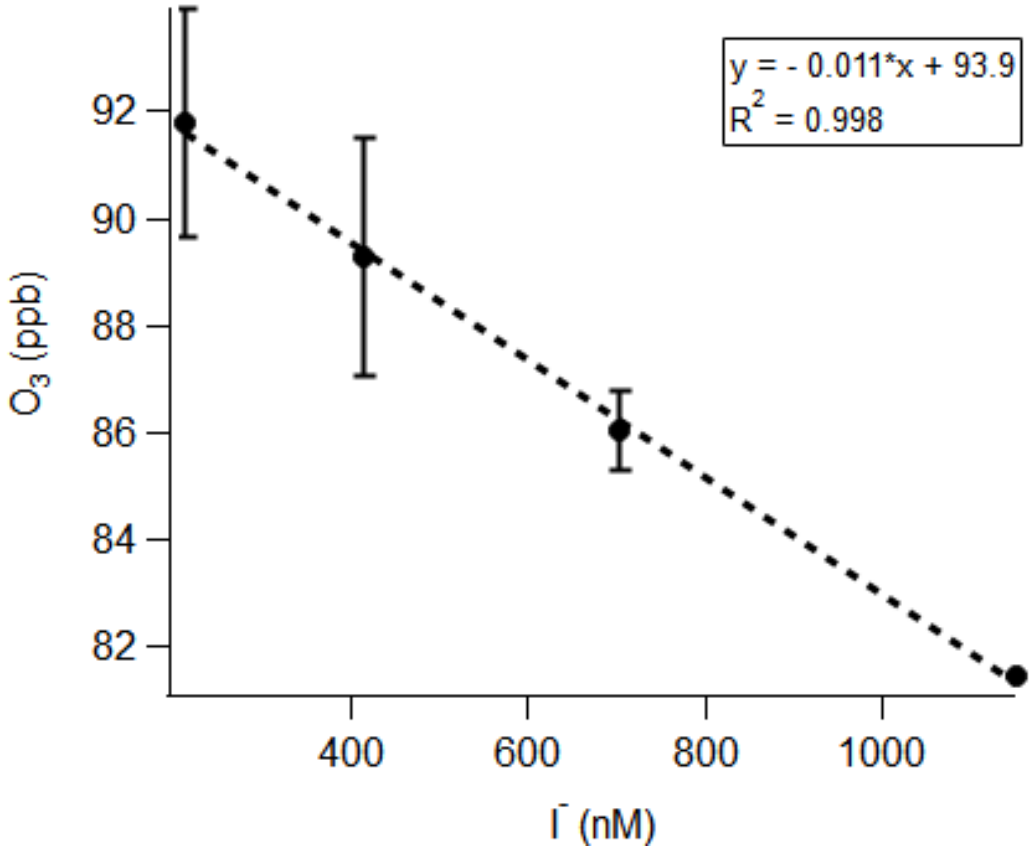

Figure S8: Calibration curve for O_3 response to changing I^- concentrations. Concentrated stock solutions were made by diluting potassium iodide (KI) (Millipore Sigma, >99% purity) into Milli-Q. Low volume concentrated solutions were added to 1 L of Milli-Q in the flow tube to produce iodide concentrations in the flow tube between 213 and 1150 nM I^-. O_3 was pushed through the flow tube at a set concentration of 92 ppb, and the resulting change in O_3 concentration from addition of I^- was monitored with a personal ozone monitor (2B Technologies). The slope of this curve is used to calculate the O_3 loss to I^- during the experiments. For 110.9 nM I^-, this results in 1.2 ppb O_3 lost to I^- after the residence time of the flow tube has been established.

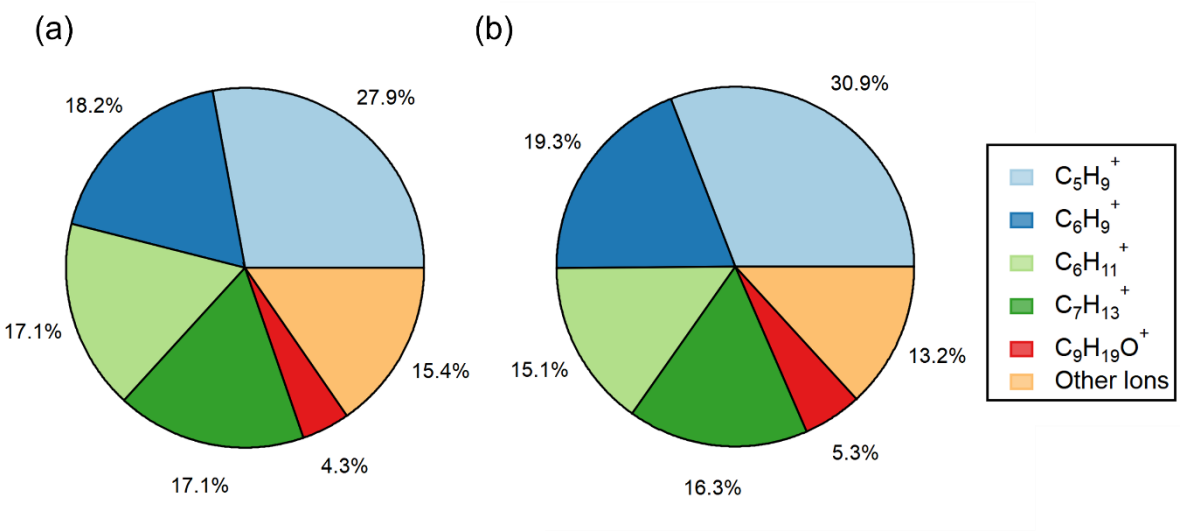

Figure S9: Distribution of ion yields to total yield when integrating from (a) 0-25 minutes and (b) 25-60 minutes according to Eq. (3).

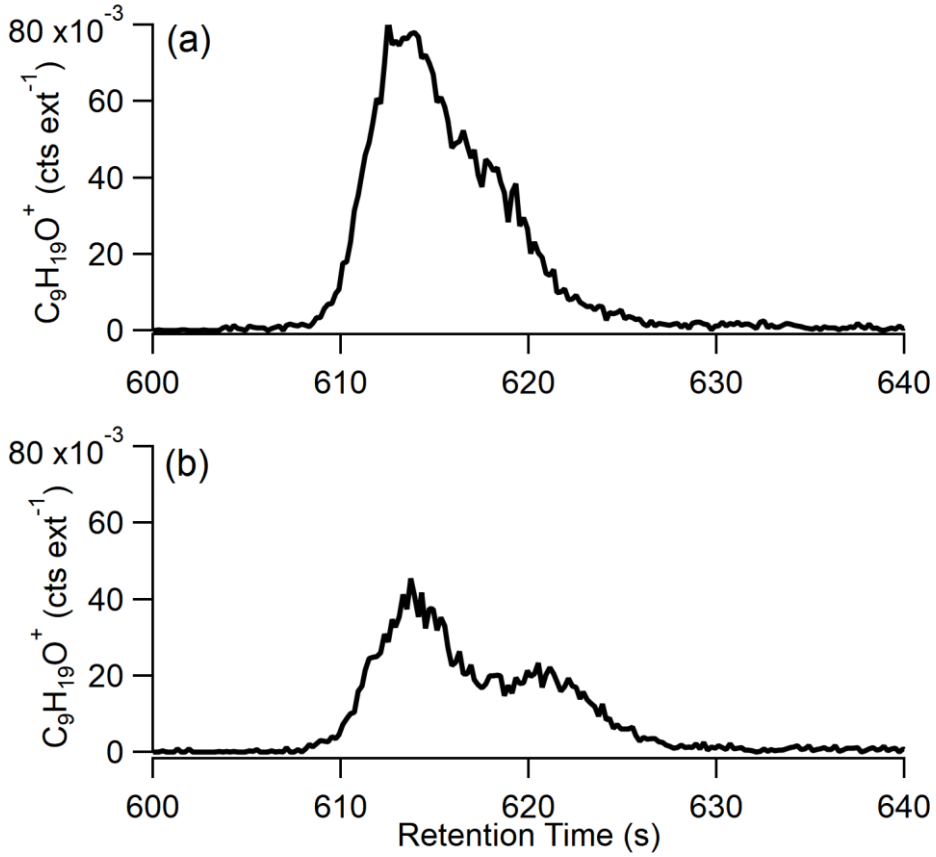

Figure S10: GC-Vocus chromatogram of $C_9H_{19}O^+$ showing that two molecules with the ion formula $C_9H_{19}O^+$ elute within 10 seconds of each other, with nonanal contributing to the rightmost peak. Based on standards and expected retention indices for this retention time, it is hypothesized that the leftmost peak is a ketone containing nine carbons. This molecule elutes close to the observed retention time of a standard of 2-nonanone, but the exact placement of the ketone group is within our retention time uncertainty, and thus is called other $C_9H_{18}O$. These two molecules are resolvable in (b) but not resolvable in (a). As a result, this peak is reported as nonanal/other $C_9H_{18}O$ in the text.

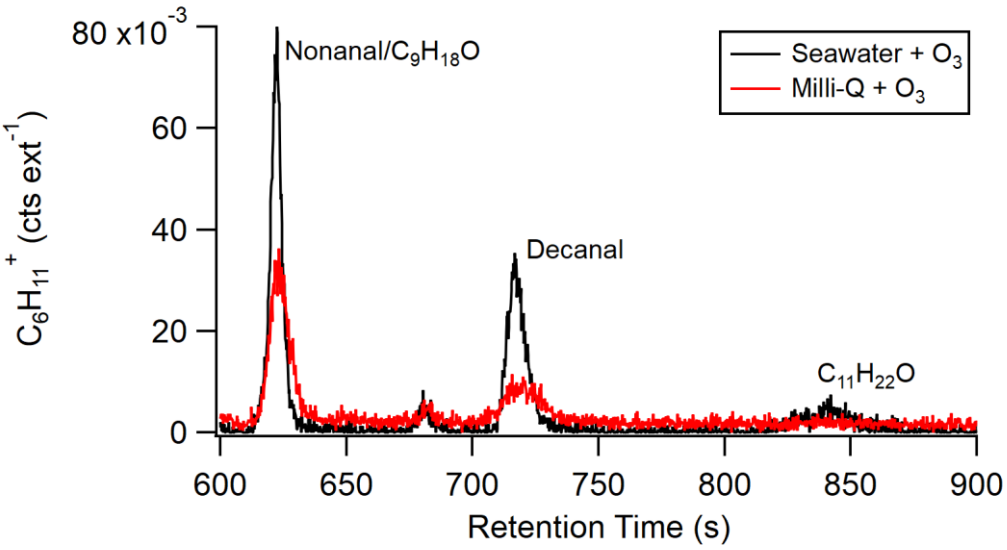

Figure S11: Example chromatograms of the $C_6H_{11}^+$ ion during ozonolysis of seawater and Milli-Q.

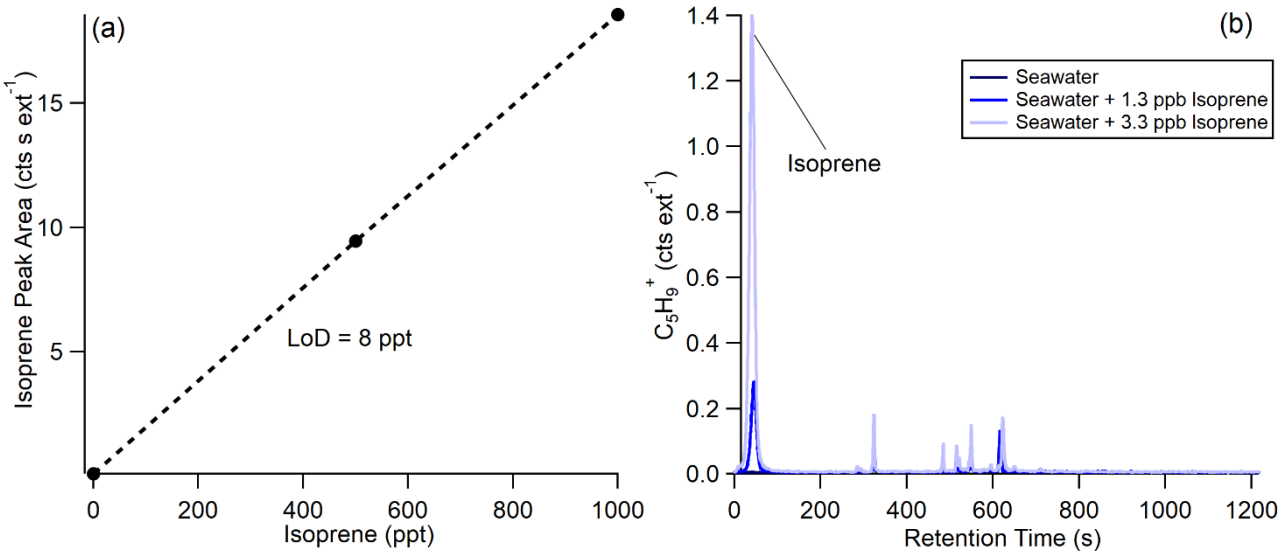

Figure S12: (a) GC-Vocus calibration curve for isoprene at 0% RH. Isoprene was delivered from the VOC mixture calibration cylinder diluted in ultrapure air. The isoprene limit of detection was 8 ppt, calculated as the full width at half maximum (FWHM) of the isoprene chromatographic peak multiplied by 3 times the standard deviation of the baseline and divided by the sensitivity, according to Claflin et al. (2021). (b) Chromatogram of $C_5H_9^+$ collected while the GC-Vocus sub-sampled from an overflow of ultrapure air through the flow tube containing seawater. Isoprene was added as standard additions from the calibration cylinder, eluting at 45 seconds in the chromatogram. This test shows the setup and instrumentation utilized can measure isoprene in the study's experimental conditions with a detection limit of 8 ppt, and the lack of isoprene observed at $C_5H_9^+$ suggests that isoprene in the study was below the detection limit.

References

Claflin, M. S., Pagonis, D., Finewax, Z., Handschy, A. V., Day, D. A., Brown, W. L., Jayne, J. T., Worsnop, D. R., Jimenez, J. L., Ziemann, P. J., de Gouw, J., and Lerner, B. M.: An in situ gas chromatograph with automatic detector switching between PTR- and EI-TOF-MS: isomer-resolved measurements of indoor air, Atmospheric Measurement Techniques, 14, 133–152, https://doi.org/10.5194/amt-14-133-2021, 2021.

Johnson, M. T.: A numerical scheme to calculate temperature and salinity dependent air-water transfer velocities for any gas, Ocean Sci., 6, 913–932, https://doi.org/10.5194/os-6-913-2010, 2010.

Kim, M. J., Novak, G. A., Zoerb, M. C., Yang, M., Blomquist, B. W., Huebert, B. J., Cappa, C. D., and Bertram, T. H.: Air-Sea exchange of biogenic volatile organic compounds and the impact on aerosol particle size distributions: Air-Sea Exchange of Biogenic VOCs, Geophysical Research Letters, 44, 3887–3896, https://doi.org/10.1002/2017GL072975, 2017.

Nightingale, P. D., Malin, G., Law, C. S., Watson, A. J., Liss, P. S., Liddicoat, M. I., Boutin, J., and Upstill-Goddard, R. C.: In situ evaluation of air-sea gas exchange parameterizations using novel conservative and volatile tracers, Global Biogeochemical Cycles, 14, 373–387, https://doi.org/10.1029/1999GB900091, 2000.

Novak, G. A., Kilgour, D. B., Jernigan, C. M., Vermeuel, M. P., and Bertram, T. H.: Oceanic emissions of dimethyl sulfide and methanethiol and their contribution to sulfur dioxide production in the marine atmosphere, Atmos. Chem. Phys., 22, 6309–6325, https://doi.org/10.5194/acp-22-6309-2022, 2022.

Sander, R.: Compilation of Henry's law constants (version 4.0) for water as solvent, Atmos. Chem. Phys., 15, 4399–4981, https://doi.org/10.5194/acp-15-4399-2015, 2015.

Shaw, S. L., Gantt, B., and Meskhidze, N.: Production and Emissions of Marine Isoprene and Monoterpenes: A Review, Advances in Meteorology, 2010, 1–24, https://doi.org/10.1155/2010/408696, 2010.